Draft version February 5, 2008
Preprint typeset using LaTeX style emulateapj v. 04/03/99

STATISTICAL PROPERTIES OF CIRCUMNUCLEAR H II REGIONS IN NEARBY GALAXIES[a]

[a]BASED ON OBSERVATIONS WITH THE NASA/ESA HUBBLE SPACE TELESCOPE, OBTAINED FROM THE DATA ARCHIVE AT THE SPACE TELESCOPE SCIENCE INSTITUTE, WHICH IS OPERATED BY THE ASSOCIATION OF UNIVERSITIES FOR RESEARCH IN ASTRONOMY, INC., UNDER NASA CONTRACT NAS 5-26555.

Almudena Alonso-Herrero
University of Hertfordshire, Department of Physical Sciences, Hatfield, Herts AL10 9AB, UK
Present address: Steward Observatory, The University of Arizona, Tucson, AZ 85721, USA

and

Johan H. Knapen
Isaac Newton Group of Telescopes, Apartado 321, E-38700 Santa Cruz de la Palma, Tenerife, Spain
and University of Hertfordshire, Department of Physical Sciences, Hatfield, Herts AL10 9AB, UK

Draft version February 5, 2008

ABSTRACT

We analyze the statistical properties of the circumnuclear H II regions of a sample of 52 nearby galaxies ($v < 1000\,\mathrm{km\,s^{-1}}$) from archival *HST*/NICMOS H-band and Paα (1.87 μm) observations at unprecedented spatial resolutions of between 1 and 30 pc. We catalog H II regions from the continuum-subtracted Paα images, and find H II regions in the central regions of most galaxies, and more than a hundred in 8 galaxies. In contrast to disk H II regions, the physical properties (luminosity and size) of individual circumnuclear H II regions do not vary strongly with the morphological type of the host galaxy, nor does the number of circumnuclear H II regions per unit area. The Hα luminosity within the central kpc, as derived from H II region emission, is significantly enhanced in early-type (S0/a–Sb) galaxies. We find evidence that bars increase the circumnuclear star formation, presumably by funneling gas from the disk towards the nucleus. Barred galaxies exhibit enhanced luminosities of the brightest H II region, the central kpc Hα luminosities (an effect mostly due to the early type galaxies in our sample), and the star formation rates per unit stellar mass (which could also be understood as the integral equivalent widths of Paα) over the central kpc with respect to non-barred galaxies.

We fit the luminosity functions and diameter distributions of the circumnuclear H II regions in 8 galaxies where we can catalog enough H II regions to do so in a meaningful way. We use power laws and find that the fitted slopes of the H II region LF are exactly in the previously found ranges, and even confirm a trend with steeper slopes in galaxies of earlier morphological type. This implies that the physical processes giving rise to enhanced star formation in the circumnuclear regions of galaxies must be similar to those in disks.

Subject headings: galaxies: ISM – ISM: HII regions – galaxies: spiral – infrared: galaxies – galaxies: irregular

1. INTRODUCTION

Extragalactic H II regions provide important clues to the physics of the star formation (SF) process because they directly trace the most massive stellar populations, and are readily observable through hydrogen recombination lines (mainly Hα). Ground-based Hα narrow-band observations of galaxies are easily obtained and allow the study of the statistics of large numbers of extragalactic H II regions (see Kennicutt 1998a for a review on the advantages and limitations of the Hα emission line for the study of SF in galaxies). H II region populations in galaxies have been studied for over 30 years now (see early review by Hodge 1974), and have been based on ever improving observational material – from photographic plates (e.g., Hodge 1969; Kennicutt, Edgar & Hodge 1989, hereafter KEH), via ground-based CCD imaging on 1-m and 2-m (e.g., Rand 1992; Banfi et al. 1993; Feinstein 1997) to 4-m class telescopes (e.g., Cepa & Beckman 1989, 1990; Knapen et al. 1993; Rozas, Beckman & Knapen 1996a; Wyder, Hodge, & Skelton 1997; Knapen 1998), to, most recently, imaging with the Hubble Space Telescope (*HST*; Pleuss, Heller, & Fricke 2000; Scoville et al. 2001; this paper).

The main results from statistical studies of more or less complete ensembles of H II regions in disks of galaxies are integral diameter distributions, and luminosity functions (LFs). The latter are usually fitted by a power-law of the form:

$$\mathrm{d}N(L) = A\,L^{\alpha}\,\mathrm{d}L \qquad (1)$$

where the index α describes the slope of the LF, and has values of $\alpha = -2.0 \pm 0.5$ for extragalactic H II regions (e.g., KEH). A similar index has been found for the LF of Galactic radio H II regions (McKee & Williams 1997, and references therein).

The most interesting features in observed H II region LFs are (1) a change in slope, with a steeper slope at the high-L end of the LF (e.g., KEH; Rand 1992; Rozas et al. 1996a; Knapen 1998), which has been explained in terms of differences in the molecular gas cloud spectrum (Rand 1992), in terms of a transition from single ionizing stars to

ionizing clusters (McKee & Williams 1997; Oey & Clarke 1998), in terms of a transition from ionization to density bounded H II regions (Beckman et al. 2000), and in terms of blending introduced by observations at too low spatial resolution (Pleuss et al. 2000); (2) steeper slopes in the interarm regions of some spiral galaxies as compared to the arm regions, observed in some galaxies (KEH; Rand 1992; Banfi et al. 1993; Thilker, Braun & Walterbos 2000; Scoville et al. 2001), but not in many others (Knapen et al. 1993; Rozas et al. 1996a; Knapen 1998); (3) a correlation between the LF slopes and the Hubble morphological type, with the slopes being systematically steeper in early-type galaxies (KEH; Banfi et al. 1993); and (4) a local maximum in the LFs around $\log L(\mathrm{H}\alpha) = 38.6 \pm 0.1$ erg s^{-1}, interpreted as evidence for a change from an ionization to a density bounded regime of H II regions of increasing luminosity by Beckman et al. (2000), but as an artifact of low resolution imaging by Pleuss et al. (2000).

From the theoretical point of view, the observational differences of H II region LFs among galaxies have been reproduced in terms of evolutionary effects (e.g., different ages, and SF histories), and properties of the ionizing clusters such as different initial mass functions (IMFs) and the maximum number of ionizing stars per cluster (e.g., von Hippel & Bothun 1990; Feinstein 1997; McKee & Williams 1997; Oey & Clark 1997, 1998; Beckman et al. 2000; Scoville et al. 2001). It is generally assumed that the shape and properties of the H II region LF directly reflect certain characteristics of the most recent SF history of the galaxy.

So far, all statistical studies of the properties of extragalactic H II regions have been performed on samples of disk H II regions, whereas the properties of nuclear and circumnuclear H II regions are relatively unknown, due to the combined effects of limited spatial resolution and blending. The central, kiloparsec scale, regions of disk galaxies, however, are interesting because of the usually increased circumnuclear or nuclear SF activity there, and because the central regions act as excellent laboratories where, e.g., SF and gas flow processes in barred and non-barred galaxies can be studied in detail (e.g., review by Knapen 1999). Even though gas fractions and star formation rates (SFRs) in the central regions can be significantly enhanced, there is as yet no convincing evidence that the SF processes in these regions are fundamentally different from those occurring in the disks of galaxies, nor for a different IMF in the central regions of galaxies, or in fact in general (e.g., reviews by Elmegreen 1998; Gilmore 2001, but see Eisenhauer 2001 for a differing view on the IMF).

We have used *HST*/NICMOS Paα images of the circumnuclear regions of a sample of 52 spiral and irregular galaxies in order to study the statistical properties of HII regions at high spatial resolution ($1 - 30$ pc). We describe the sample, data, and production of the HII region catalogs in Section 2, and the statistical properties of the HII regions in Section 3 and 4. We discuss our results and summarize our conclusions in Section 5.

2. THE DATA

2.1. *The sample*

We have selected a sample of galaxies from the *HST*/NICMOS Paα snapshot survey of nearby galaxies as published by Böker et al. (1999), imposing the criteria that galaxies have morphological type S0/a or later, and velocities of $v < 1000$ km s^{-1}. The Böker et al. (1999) "snapshot" survey consists of galaxies selected at random from a master list taken from the Revised Shapley Ames Catalog (RSA) according to *HST* scheduling convenience. Our sample contains a total of 52 galaxies, and is presented in Table 1, which lists the Hubble type, heliocentric velocity from the Nearby Galaxies Catalog (Tully 1988), morphological type, and the distance from the Tully (1988) catalog assuming $H_0 = 75$ km s^{-1} Mpc^{-1}.

In terms of the morphological type, 25% of the sample are galaxies with $T = 0 - 3$ (that is, morphological types earlier than Sbc), 19% are galaxies with $T = 4{-}5$ (Sbc–Sc) and 56% galaxies with types $T > 5$ (morphological types later than Sc). According to the presence or absence of a bar the sample is divided into: 40% unbarred (A), 25% strongly barred (B) and 35% weakly barred (AB).

We determined whether there are distance biases within these subclasses, and found that the weakly barred galaxies are at slightly larger distances: galaxies with type AB are at a median distance of 9.7 Mpc, unbarred galaxies at 5.6 Mpc, and strongly barred galaxies at 7.5 Mpc. We also found that the early-type galaxies in our sample are more distant: $T = 0 - 3$ are at a median distance of 14.5 Mpc, whereas $T = 4 - 5$ and $T > 5$ are at median distances of 9.5 Mpc and 7.5 Mpc, respectively. These biases are accounted for when we analyze properties dependent on the distance, as detailed below.

2.2. *Observations and Data Reduction*

Images were taken with the NIC3 camera (pixel size $0.2''$ pixel^{-1}) of NICMOS on the *HST* using the broad-band F160W filter (equivalent to a ground-based H-band filter), and the narrow-band F187N filter. The latter filter ($\Delta\lambda/\lambda \simeq 1\%$) contains the emission line of Paα and the adjacent continuum at 1.87 μm. The field of view of the images is $51.2'' \times 51.2''$, which in our galaxies corresponds to the central 175 pc $-$ 5 kpc, depending upon the distance to the galaxy.

The images were reduced following standard procedures (see Alonso-Herrero et al. 2000 for more details). The angular resolution (FWHM) of the NIC3 images is $0.3''$, as measured from the point spread function (PSF) of stars in the images. This corresponds to typical spatial resolutions of between 1 pc and 30 pc for the galaxies in our sample, using the distances given in Table 1.

The flux calibration of the F160W and F187N images was performed using conversion factors based upon measurements of the standard star P330-E, taken during the Servicing Mission Observatory Verification (SMOV) program (M. J. Rieke, private communication 1999). Unfortunately, there are no observations available of the continuum adjacent to Paα, so we used the flux calibrated images at 1.6 μm as continuum for the F187N images. As discussed in Maiolino et al. (2000), ideally narrow-band continuum images on both sides of the emission line are needed to perform an accurate continuum subtraction which takes into account the spatial distribution of the extinction. We fine-tuned the scaling of the continuum image so that the continuum subtracted Paα image (flux calibrated) did not show negative values. This method generally produces satisfactory results, except in those

TABLE 1
THE SAMPLE.

Galaxy	Hubble type	Morphological type	v (km s^{-1})	Tully distance
NGC 247	7	SAB(s)d	159	2.1
NGC 598	6	SA(s)cd	−182	0.7
NGC 628	5	SA(s)c	659	9.7
NGC 672	6	SB(s)cd	425	7.5
NGC 891	3	SA(s)b?	529	9.6
NGC 925	7	SB(s)c	554	9.4
NGC 2366	10	IB(s)m	102	2.9
NGC 2403	6	SAB(s)cd	132	4.2
NGC 2681	0	(R')SAB(rs)0/a	710	13.3
NGC 2683	3	SA(rs)b	415	5.7
NGC 2841	3	SA(r)b	637	12.0
NGC 2903	4	SB(s)d	554	6.3
NGC 2976	5	SAcpec	9	2.1
NGC 3077	13	I0pec	10	2.1
NGC 3184	6	SAB(rs)cd	599	8.7
NGC 3593	0	SA(s)0/a	628	5.5
NGC 3627	3	SAB(s)b	737	6.6
NGC 3675	3	SA(s)b	771	12.8
NGC 3738	10	Irr	225	4.3
NGC 3769	3	SB(r)b	714	17.0
NGC 3782	6	SAB(s)cd	740	17.0
IC 749	6	SAB(rs)cd	784	17.0
IC 750	2	Sab	713	17.0
NGC 4062	5	SA(s)c	769	9.7
NGC 4085	5	SAB(s)c	714	17.0
NGC 4102	3	SAB(s)b	862	17.0
NGC 4136	5	SAB(s)c	618	9.7
NGC 4144	6	SAB(s)cd	267	4.1
NGC 4178	8	SB(rs)dm	381	16.8
NGC 4183	6	SA(s)cd	934	17.0
NGC 4190	10	Impec	234	2.8
NGC 4192	2	SAB(s)ab	−142	16.8
NGC 4293	0	(R)SB(s)0/a	882	17.0
NGC 4294	6	SB(rs)cd	415	16.8
NGC 4299	7	SAB(s)dm	238	16.8
NGC 4389	6	SB(rs)bc	718	17.0
NGC 4395	9	SAd	318	3.6
NGC 4449	10	IBm	200	3.0
NGC 4559	6	SAB(rs)cd	816	9.7
NGC 4571	6	SA(r)d	348	16.8
NGC 4605	5	SB(s)c pec	140	4.0
NGC 4701	6	SA(s)cd	727	20.5
NGC 4826	2	(R)SA(rs)ab	414	4.1
NGC 5055	4	SA(rs)bc	497	7.2
NGC 5474	6	SA(s)cd	277	6.0
NGC 5585	7	SAB(s)d	303	7.0
IC 5052	7	SBd	598	6.7
NGC 6207	5	SA(s)c	852	17.4
IC 4710	9	SB(s)m	741	8.9
NGC 6744	4	SAB(r)bc	842	10.4
NGC 6822	10	Im	−56	0.7
NGC 6946	6	SAB(rs)cd	46	5.5

cases where the differential extinction between 1.60 μm and 1.87 μm is significant (typically edge-on galaxies and the nuclei of some galaxies). As we shall see in the next section, the H II region photometry software takes into account the local background, so the continuum subtraction is not a dominant source of error, although errors associated with the background subtraction depend on the luminosity of the H II region.

Throughout the paper we have converted the Paα luminosity into the more commonly used Hα luminosity, assuming case B recombination ($\frac{\mathrm{H}\alpha}{\mathrm{Pa}\alpha} = 8.7$). We also stress that the effects of reddening in the central regions will be attenuated with the use of Paα luminosities with respect to Hα luminosities ($A(\mathrm{Pa}\alpha) \simeq 0.2\,A(\mathrm{H}\alpha)$; Rieke & Lebofsky 1985).

2.3. *Production of the H II region catalogs*

The H II region catalogs were produced using the software REGION, kindly provided by Dr. C. H. Heller (see Pleuss et al. 2000, and references therein for a detailed description). REGION is a semi-automated method to locate and compute statistics of H II regions in an image, based on contouring, and taking into account the local background. The lower limit for the size of an H II region is set to 9 contiguous pixels, which corresponds to *minimum* linear sizes of between 2 and 60 pc. Each pixel must have an intensity above the local background of at least three times the rms noise of that local background (see Rand 1992 and Knapen et al. 1993 for more details on the criteria employed). After identifying the H II regions, the program measures their position, size (area) and luminosity by subtracting the closest local background from the observed flux. For those galaxies with detected H II regions, in Table 2 we list the number of H II regions identified, the Hα luminosity of the brightest, faintest, and median H II, as well as the diameter of the largest and median H II region. A total of 10 galaxies were excluded from most of the H II region analyses for various reasons, as detailed in the footnote to Table 2

There are two methods to define the extent of an H II region: percentage-of-peak photometry (PPP) and fixed-threshold photometry (FTP). The former defines the area to be assigned to an H II region within an isophote whose brightness is a fixed percentage of the intensity peak, and avoids problems of S/N at the boundary of the region. The latter uses a limiting surface brightness method to define an H II region (see Kingsburgh & McCall 1998 for a detailed comparison of the two methods).

We used the FTP method, but we still needed to impose the condition of a minimum size (in pixels) for identifying an H II region. Thus for galaxies at different distances this corresponds to differing *minimum* physical sizes. This effect can be clearly seen in the median diameters (in pc) of the detected H II regions found for each galaxy (Table 2). In order to show the effect of distance on the derived properties, the galaxies in Table 2 are sorted by increasing distance.

3. STATISTICAL PROPERTIES

3.1. *Resolution effects*

One of the most important issues when analyzing the properties of the HII region LF is the role of observational parameters, especially spatial resolution. Until now, most HII region LFs were based upon ground-based Hα imaging with spatial resolutions ranging from 0.8 to a few arcsec, or from 5 pc (in M31; Walterbos & Braun 1992) to a few hundred pc (KEH; Rand 1992; Knapen et al. 1993; Banfi et al. 1993; Rozas et al. 1996a, Knapen 1998), depending upon the distance of the galaxy. Rand (1992) discussed the effects of blending on the properties of the HII region LF. Such blending, e.g., in the case where a smaller H II region is spatially coincident with a larger one and is not cataloged, is expected to occur more frequently as the spatial resolution decreases. Rand (1992) concluded from his modeling of this problem that blending does not significantly affect the measured slope of the H II region LF as determined from his ground-based image of M51.

More recently, Pleuss et al. (2000) specifically studied the impact of different spatial resolution on, among other parameters, the diameter distribution and LF of H II regions. They used *HST* archive Hα images of selected areas of the spiral galaxy M101, and degraded these to a typical ground-based resolution of 0.8 arcsec (FWHM). The linear scales sampled by their high and low resolution images were 3.6 and 77.6 pc/pixel, respectively. Although the integral diameter distributions of the H II regions are significantly different at high and low resolution (as expected, see Knapen 1998), the LF slopes are only slightly different, being shallower in the low resolution case. A similar effect is found by Scoville et al. (2001) who compared their *HST* (both WFPC2 and NICMOS) H II region LF with that of Rand (1992) for M51, with the high-resolution LF significantly steeper than the low-resolution one. Not only are the fitted slopes quite different but the methods used to arrive at them, so the comparison is less direct than in the work by Pleuss et al. and Rand. It must be kept in mind that the use of higher spatial resolution imaging also introduces some problems. For instance, H II regions may be over-resolved, and individual components or stars within what ought to be considered one single H II region may be cataloged as separate, and by implication smaller and less luminous, ones.

It is outside the scope of the current paper to discuss in detail the problems of resolution on the statistical results on ensembles of H II regions in spiral galaxies. However, we do briefly summarize a few basic considerations which give some idea of physical scales. Firstly, consider the ideal case of a Strömgren sphere, where the radius of an H II region can be approximated in terms of the number of ionizing photons and a number of factors which depend on the electron temperature and density (see e.g., Strömgren 1939; Osterbrock 1989). One finds that the radius of the Strömgren sphere of a main sequence O5 star is 108 pc, whereas that of a B0.5 star would be 12 pc (Osterbrock 1989). In sites of strong SF, massive stars tend to be clustered in OB associations, so the expected sizes of the H II regions ionized by these associations would be of the order of a few hundred pc. Secondly, Walterbos & Braun (1992) estimate an upper limit for the Hα luminosity of planetary nebulae (PN) in M31 of $4 \times 10^{35}\,\mathrm{erg\,s^{-1}}$. For comparison, the H$\alpha$ luminosity for H II regions ionized by an O5 star is $6 \times 10^{37}\,\mathrm{erg\,s^{-1}}$ (this corresponds to the approximate limit of an H II region ionized by a single star or multiple stars), whereas for a B0.5 star it is $1 \times 10^{35}\,\mathrm{erg\,s^{-1}}$. The median H$\alpha$ luminosities of NGC 598 and NGC 6207, the

TABLE 2
STATISTICAL PROPERTIES OF CIRCUMNUCLEAR H II REGIONS IN GALAXIES.

Galaxy	Dist (Mpc)	no H II	$\log L_{\rm br}$(Hα) (erg s^{-1})	$\log L_{\rm f}$(Hα) (erg s^{-1})	$\log L_{\rm med}$(Hα) (erg s^{-1})	diam$_{\rm med}$ (pc)	diam$_{\rm lar}$ (pc)	$\log L_{\rm kpc}$(Hα) (erg s^{-1})	$M_{\rm F160W}$
(1)	(2)	(3)	(4)	(5)	(6)	(7)	(8)	(9)	(10)
NGC 598	0.7	65	36.74	35.28	35.62	3	9	...	...
NGC 6822	0.7	4	35.98	35.64	35.70	3	4	...	...
NGC 2976	2.1	17	37.47	36.17	36.62	11	24	...	...
NGC 3077	2.1	155	38.30	36.12	36.79	10	28	...	...
NGC 4190	2.8	5	36.78	36.17	36.55	13	16	...	...
NGC 2366	2.9	3	36.70	36.44	36.62	12	13	...	...
NGC 4449	3.0	155	38.32	36.39	36.90	14	36	39.50	-18.39
NGC 4605	4.0	40	37.92	36.50	36.98	17	47	38.84	-18.88
NGC 4144	4.1	7	38.17	37.05	37.30	14	31	38.43	-17.77
NGC 4826	4.1	184	38.34	36.86	37.26	16	45	39.72	-20.95
NGC 2403	4.2	39	37.98	36.69	36.92	17	46	38.71	-19.55
NGC 3738	4.3	52	38.35	36.50	37.05	21	72	39.10	-18.08
NGC 3593	5.5	103	38.77	37.09	37.81	26	59	40.05	-19.98
NGC 6946	5.5	252	39.80	36.84	37.39	25	93	40.33	-19.45
NGC 5474	6.0	12	37.62	36.89	37.09	22	35	38.25	-18.00
NGC 2903	6.3	111	39.42	37.02	38.35	28	101	40.34	-20.58
NGC 3627*	6.6	28	38.47	36.24	37.67	26	48	39.69	-21.02
IC 5052	6.7	14	39.24	37.39	37.94	36	97	39.52	-17.51
NGC 5585	7.0	8	37.80	36.98	37.50	29	42	38.08	-17.88
NGC 5055	7.2	100	38.24	37.22	37.54	27	51	39.32	-20.59
NGC 672	7.5	34	38.47	36.98	37.26	30	72	39.01	-18.26
NGC 3184*	8.7	19	38.77	37.22	37.70	39	69	39.27	-18.15
NGC 925	9.4	17	38.89	37.46	37.81	41	78	38.50	-18.45
NGC 628	9.7	13	38.30	37.54	37.80	38	52	38.77	-19.77
NGC 4062	9.7	25	38.02	37.28	37.55	36	59	38.39	-19.22
NGC 4559	9.7	20	38.89	37.89	38.09	38	69	39.20	-19.10
NGC 4136	9.7	23	38.19	37.12	37.32	35	55	38.29	-18.26
NGC 3675	12.8	68	38.51	37.57	37.86	49	89	40.03	-21.12
NGC 4178	16.8	24	39.34	37.86	38.32	70	206	39.36	-18.62
NGC 4192	16.8	44	39.52	37.88	38.52	76	158	40.36	-21.44
NGC 4294	16.8	60	39.34	37.85	38.30	76	160	39.38	-18.59
NGC 4299	16.8	39	39.52	37.83	38.34	74	192	39.44	-17.77
NGC 3769	17.0	35	39.17	37.84	38.14	67	157	39.74	-19.56
NGC 3782	17.0	25	39.14	37.72	38.17	74	145	38.27	-18.32
IC 749	17.0	20	38.61	37.75	37.98	66	115	38.49	-18.21
IC 750	17.0	156	39.89	38.17	38.62	72	192	40.73	-21.19
NGC 4085*	17.0	43	39.56	38.24	38.43	64	143	40.13	-19.83
NGC 4102*	17.0	36	40.24	37.84	38.32	80	228	40.94	-21.91
NGC 4183	17.0	6	38.80	37.89	38.12	68	95	39.11	-18.65
NGC 4389	17.0	21	39.44	38.32	38.70	74	151	40.11	-19.18
NGC 6207	17.4	58	39.80	37.86	38.34	82	283	38.96	-19.47
NGC 4701	20.5	48	39.47	37.98	38.30	80	249	39.50	-19.52

NOTE.—(1): Name of galaxy. (2): Distance. (3): Number of H II regions identified. (4), (5) and (6): Hα luminosity of the brightest, faintest and median H II region. (7) and (8): diameter of largest and median H II region. (9) and (10): Hα luminosity in H II regions and absolute F160W (H-band) magnitude over the central kpc.
* Nuclear emission excluded from H II region statistics (columns (3) through (8)).
Galaxies excluded from the statistical analysis of H II regions: NGC 247 (faint), NGC 891 (dust and edge-on) NGC 2681 (nuclear emission only), NGC 2683 (dust and edge-on), NGC 2841 (nuclear emission only), NGC 4293 (nuclear emission only and dust) NGC 4395 (nuclear emission only), NGC 4571 (faint), IC 4710 (nuclear emission only) and NGC 6744 (nuclear emission only).

closest galaxies in our sample, are 4 and $5 \times 10^{35}\,\mathrm{erg\,s^{-1}}$, respectively, or close to the limit for PN, and we have thus excluded these two galaxies from our statistical analysis. For the remaining galaxies, the Hα luminosities of the detected H II regions are always above the limit of PN, so they are likely to correspond to real H II regions.

3.2. *Number of H II regions*

KEH analyzed the properties of disk H II regions of a sample of nearby spiral and irregular galaxies. They found that the number of H II regions (normalized to the total B-band luminosity) increases by a factor of 6 from Hubble type Sb to Sc, and by another 50% from Sc to irregulars. KEH observed a similar behavior with the number of H II regions per unit area, and no significant differences between the H II regions in the inner and outer halves of the disk of a given galaxy.

From Table 2, it can be seen that within a given distance bin, there is a large dispersion in the number of H II regions detected in the circumnuclear regions of galaxies. We can determine whether there is a relation between the number of central H II regions per unit area in kpc^2 (so the distance effect on the region covered by the images can be attenuated) and the morphological type (we use the types T given in Table 1) for all galaxies. The comparison is presented in the upper left panel of Figure 1, where galaxies have been divided into three morphological groups: $T = 0-3$, $T = 4-5$ and $T > 5$. We only include galaxies with distances $d \geq 2\,\mathrm{Mpc}$, and plot galaxies with only nuclear emission (see notes of Table 2) as having one H II region detected. We also indicate the value of the median of the distribution. This diagram does not show the tendency for later-type galaxies to have more circumnuclear H II regions per unit area than the earlier types, found by KEH for H II regions in the disks of galaxies.

In the upper right panel of Figure 1, we compare a related quantity, that is the number of H II regions per unit near-infrared H-band luminosity, which represents the stellar mass in the region covered by the images. From this figure it can be seen that although the values of the median only rise slowly from early to late types, the late-type galaxies show a tail in the distribution reaching higher numbers of circumnuclear H II regions per unit stellar mass than earlier-types. This is caused by the fact that early morphological type galaxies tend to have more luminous (and more massive) bulges. This in good agreement with the global behavior of disk H II regions in nearby galaxies (KEH).

A similar comparison is carried out using the bar class (A, AB and B) to determine whether the presence of a bar in a galaxy influences the number of circumnuclear H II regions. The comparison is shown in the lower panels of Figure 1 for the number of H II regions per unit area, and per unit stellar mass. There is no tendency for barred galaxies to show more H II regions per unit stellar mass or unit area.

3.3. *H II region luminosities*

The accepted view is that the global SF activity in galaxies decreases systematically from late-type to early-type spirals, a conclusion mainly based on the integrated equivalent widths of Hα (e.g., Kennicutt & Kent 1983 and Kennicutt 1998a for a review). This view is also supported by the fact that the luminosities of the brightest H II regions in the disks of early-type spiral galaxies are on average lower than those of later types (KEH). Moreover, Caldwell et al. (1991) reported that in Sa galaxies there are no H II regions with Hα luminosities greater than $10^{39}\,\mathrm{erg\,s^{-1}}$, although this view has been challenged by Devereux & Hameed (1997) and Hameed & Devereux (1999, and references therein). The SF activity of galaxy nuclei differs from the global behavior as found by Ho, Filippenko, & Sargent (1997a) who from an optical spectroscopic survey showed that early-type (S0–Sbc) galaxies have nuclei with higher Hα luminosities than late-type (Sc–I0) galaxies, with an increase in the median of about a factor of 9, for H II (starburst) type galaxies.

When we compare the median luminosities of the circumnuclear H II regions with the morphological type for galaxies within distance bins (see Table 2), we find no clear evidence for later-type galaxies to show brighter circumnuclear H II regions. For instance, within the $d = 17\,\mathrm{Mpc}$ distance bin, the median Hα luminosity of H II regions in the early-type spirals IC 750 and NGC 4192 are above the average value within this bin (although we note that IC 750 is an interacting galaxy). A similar behavior is found within the 4–5 Mpc distance bin, where the early-type galaxies NGC 3593 and NGC 4826 host relatively bright median H II regions. Although our number of early-type spirals (that is, Sa and Sab) is small, there is no clear trend for earlier-type galaxies to show fainter circumnuclear H II regions.

The luminosity of the brightest circumnuclear H II region can be used as an estimate of the age of the SF process (at least if the SF occurred in an instantaneous burst), although this quantity is also dependent upon the maximum number of ionizing stars per cluster, and upon the upper mass cutoff of the IMF (see Feinstein 1997; Oey & Clark 1998). An advantage of using the luminosity of the brightest H II region over the mean luminosity is that is not sensitive to the minimum size imposed for the detection of an H II region, although the blending effects will be more important for the more distant galaxies.

The left panel of Figure 2 shows the logarithm of the Hα luminosity of the brightest circumnuclear H II region as a function of morphological type (grouped as in Figure 1) for galaxies with distances $d > 2\,\mathrm{Mpc}$. For a given group of morphological types, there is a spread of approximately two orders of magnitude in the luminosity of the brightest H II region, where part of the scatter is probably caused by blending effects in the more distant galaxies. Although the median values of the Hα luminosity for the brightest H II region are similar for the early-types ($T = 0-3$) and late type ($T > 5$), the distribution for the late-type galaxies shows a tail reaching fainter luminosities. As the early-type galaxies are biased towards more distant galaxies, we checked that the low luminosity tail in the late types is not caused by the distance effect by examining the distribution excluding galaxies with distances $d \geq 12\,\mathrm{Mpc}$. Again we find no tendency for the late type ($T > 5$) galaxies to show more luminous brightest H II regions than their early type counterparts.

This result is in clear contrast with the behavior of disk H II regions. Kennicutt (1988) found that the brightest H II regions in irregular galaxies are approximately 6 times

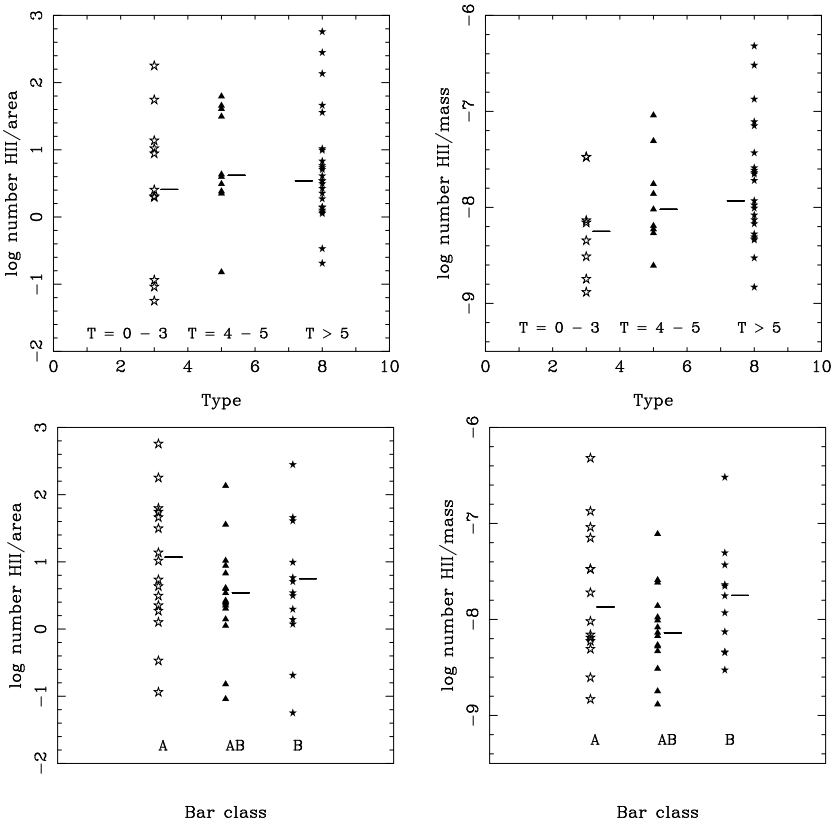

FIG. 1.— *Upper left panel:* Distribution of the number of H II regions per unit area for types $T = 0 - 3$, $T = 4 - 5$ and $T > 5$ (given in Table 1). *Upper right panel:* Same as left panel but with number of H II regions per stellar mass unit (as traced by the H-band luminosity). *Lower panels:* Same as upper panels but comparing with the bar class. All diagrams are for galaxies with distances $d \geq 2$ Mpc. The horizontal ticks next to the symbols show the median value of the distribution.

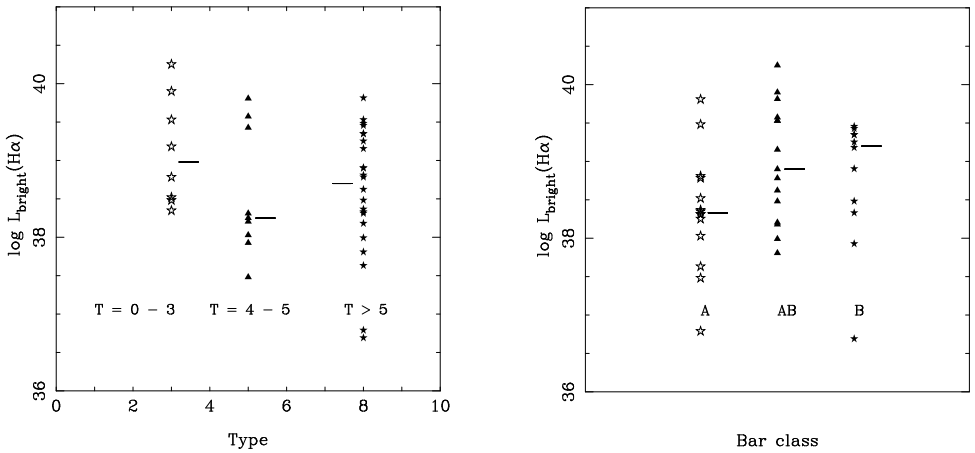

FIG. 2.— Hα luminosity of the brightest H II region as a function of the morphological type (left panel) and bar class (right panel) for those galaxies in our sample with distances $d \geq 2$ Mpc.

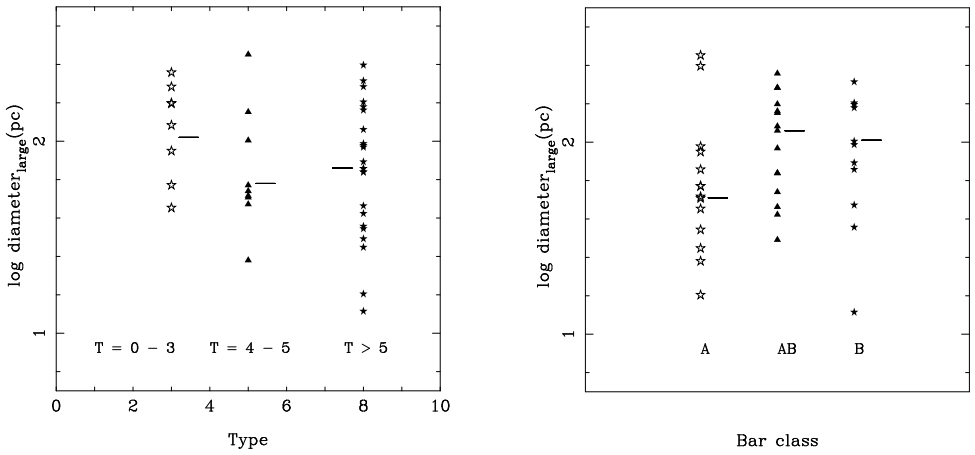

FIG. 3.— As Figure 2, but for the diameter of the largest H II region.

brighter than those in Sbc-Sc galaxies of the same absolute blue magnitude, and approximately 50 times brighter than their counterparts in Sab–Sb galaxies. This result is always referred to disk H II regions. Moreover, three of the six galaxies in our sample with Hubble morphological types S0/a to Sab show $L_{\rm br}(\rm H\alpha)$ near or above the limit given in Caldwell et al. (1991), whereas two only show faint central emission. Although the numbers are small, it is evident that some early-type galaxies can harbor very luminous central H II regions. Possible explanations for these discrepant results are resolution effects, reduced extinction in our Paα data, but more likely a different behavior of circumnuclear H II regions versus disk H II regions.

The bar potential in a disk galaxy, which by its non-axisymmetric nature can funnel gaseous material from the disk inwards toward the central regions, is usually invoked as a triggering of the SF in the centers of galaxies (e.g., Shlosman, Begelman & Frank 1990). There, the gas can accumulate, possibly near one or more inner Lindblad resonances, become gravitationally unstable, and this can lead to enhanced massive star formation.

We can now check this scenario by comparing the luminosity of the brightest H II region with the bar class (right panel of Figure 2). There is a clear tendency for barred galaxies to show more luminous brightest H II regions than their unbarred counterparts, as can be seen from the increasing value of the median of the brightest H II region distribution from unbarred (A) to strongly barred (B) galaxies. Although the median distance of the strongly barred galaxies is higher than that of unbarred galaxies, the distance effect alone is not enough to account for the differing medians of the distributions of the brightest H II regions. If galaxies in the Virgo cluster, which populate 40% of the strongly barred galaxy bin and 50% of the weakly barred galaxy bin, are excluded, we find that the median of the distribution of the brightest H II regions in barred galaxies (AB+B) is slightly higher than in unbarred galaxies, but on average the brightest H II regions in barred galaxies are a factor of five brighter than those in unbarred systems. A K-S test shows that there is only a probability of $P_{\rm K-S} = 0.11$ that both distributions are drawn from the same population, for galaxies with $d < 12$ Mpc. The scenario described above is proven here in a statistical and qualitative way, a conclusion that fits in well with the long known preference for central starburst galaxies to be barred (e.g., Heckman 1980; Balzano 1983; Devereux 1987), and with the occurrence of circumnuclear ring-like regions of much enhanced SF in barred galaxies (Knapen 1999).

3.4. *H II region sizes*

The size of an H II region is not as easy to measure as its luminosity, because the former quantity is observationally mostly influenced by pixels at the perimeter of the H II region, thus maximizing the sensitivity to blending and background noise, whereas the luminosity is determined mostly by the bright pixels near the centers of H II regions. Nevertheless, Hodge (1986) found that late-type galaxies (Sc and Irr) tend to have larger H II regions than early-type galaxies. Kennicutt (1988) measured the sizes of the first ranked H II regions in a sample of spiral and irregular galaxies, and reached a similar conclusion, although the trend was not as significant as for the luminosity of the brightest H II regions.

In Figure 3 (see also Table 2) we compare the size of the largest H II region (which is not necessarily the brightest one) with the morphological type and bar class. As found with the luminosity of the brightest H II region, there is no clear trend with the morphological type. The size of the largest H II regions in barred galaxies is on average larger than for unbarred galaxies. As we did for the luminosity of the brightest H II region, if the distribution is examined only considering galaxies with distances $d < 12$ Mpc (to avoid distance biases), the trend is maintained with a probability of only $P_{\rm K-S} = 0.16$ that the size distributions of the largest H II region in barred and unbarred galaxies are drawn from the same population.

In summary, we can state that while the physical properties (luminosity and size) of the circumnuclear H II regions are less sensitive to the morphological type of their

host galaxy than those of disk H II regions, the presence of a bar produces on average larger and more luminous circumnuclear H II regions than in non-barred galaxies.

3.5. *Central kpc Hα luminosities and specific SFRs*

The use of narrow band Paα imaging, as opposed to spectroscopy, allows to evaluate the strength of the SF activity in the centers of galaxies, covering the same physical size for all galaxies. For this purpose, we use two quantities, the total Hα emission (only from H II regions) and the SFR per stellar mass unit (also known as specific SFR). The SFR per unit stellar mass can also be understood as an integrated pseudo equivalent width of Paα, since both are basically the result of dividing the Paα flux by the nearby H-band continuum. Thus, the specific SFR or the pseudo equivalent width can be used as an estimate of the efficiency of the SF processes with respect to the stellar mass, the age of the SF process, or most likely, a combination of both.

We evaluated the Hα luminosity and specific SFR for the central kpc of each galaxy in our sample except for those with distances of less than 4 Mpc as the NIC3 field of view does not cover the central kpc. The Hα emission was calculated by adding the luminosity of all the H II regions whose centers are within the central circular kpc area. We performed aperture photometry (circular apertures) covering the central kpc on the H-band images, and used the mass-to-light ratio given in Thronson & Greenhouse (1988) to estimate the central stellar masses. The Hα luminosities and absolute H-band magnitudes over the central kpc for the galaxies in our sample are listed in the last two columns of Table 2. The SFRs are computed using the relation provided in Kennicutt (1998b). Note that these quantities are obviously independent of the distance of the galaxy, and resolution effects.

The comparison of the central Hα luminosity with the morphological type is presented in the left panel of Figure 4, which clearly shows enhanced SF in the central kpc of early type galaxies. This confirms the tendency found by Böker et al. (1999) of higher average surface brightnesses (over the field of view of the images) for earlier morphological types, as well as results by Ho et al. (1997a,b) from optical spectroscopy. However, when the specific SFRs are plotted versus the morphological type there is no clear increase of the specific SFRs for earlier type galaxies, mainly because these galaxies tend to have more massive bulges (Figure 5, left panel).

The effect of a bar on both the central kpc Hα luminosity and specific SFRs is evaluated in the right panels of Figure 4 and 5. The distributions of the central kpc Hα luminosities (only in H II regions) show slightly increasing values of the median from unbarred to barred galaxies. However, as also found by Ho et al. (1997b) using optical spectroscopy (although their spectroscopy did not cover the same physical size for all galaxies), the distribution for barred (AB+B) galaxies has a tail reaching higher central Hα luminosities ($\log L(\mathrm{H}\alpha)_{\mathrm{kpc}} > 40\,\mathrm{erg\,s^{-1}}$) than that of unbarred galaxies. This result is not of a high statistical significance, with a probability that the distributions of central Hα luminosity of barred and unbarred galaxies are drawn from the same population of $P_{\mathrm{K-S}} = 0.33$. Ho et al. (1997b) noted that the trend for barred galaxies to show enhanced central SF was more prominent if only early-type (S0/a–Sbc) were considered. We reexamined their result but with all galaxies covering the same physical size (the central kpc). Although this subsequent subdivision of our sample implies small number statistics, we find significant differences, with early type ($T < 5$) unbarred galaxies showing a median of $\log L(\mathrm{H}\alpha)_{\mathrm{kpc}} = 39.3\,\mathrm{erg\,s^{-1}}$ (7 galaxies) in contrast with their barred counterparts: $\log L(\mathrm{H}\alpha)_{\mathrm{kpc}} = 40.1\,\mathrm{erg\,s^{-1}}$ (9 galaxies). On the other hand, the late type galaxies, both barred and unbarred, show similar values of the median of the distributions: $\log L(\mathrm{H}\alpha)_{\mathrm{kpc}} = 39.2\,\mathrm{erg\,s^{-1}}$. Clearly, the luminosity enhancement in the central kpc of barred galaxies occurs almost entirely in early type galaxies.

We also find enhanced specific SFRs (or pseudo equivalent widths of Paα) in the central kpc of barred galaxies as seen from the increasing median of the distributions from unbarred to barred galaxies (see right panel of Figure 5). This is in good agreement with findings by Ho et al. (1997b) who used the equivalent width of Hα. This provides further evidence in support of the expected enhancement of SF (both in terms of the efficiency and the younger ages) in the centers of barred with respect to non-barred galaxies, due to gas losing angular momentum in a bar, and falling inward from the disk to the central region.

4. LFS AND DIAMETER DISTRIBUTIONS

In this section we concentrate on those galaxies for which we cataloged 100 or more H II regions from the Paα images of the circumnuclear regions, and for which we can construct reliable LFs and integral diameter distributions.

4.1. *H II region LFs*

The differential LFs of circumnuclear H II regions for the selected galaxies are presented in Figure 6, as log-log plots in luminosity bins of 0.20 dex. We also show the best fit to the slope (with $\alpha = \mathrm{slope} - 1$) in the figures. The parameters of the fit to the circumnuclear H II region LF (α and the luminosity range used for fitting the slope) are given in Table 3. The slopes of the LFs are very much within the range found for LFs for disks of spiral galaxies from ground-based imaging, perhaps surprisingly so given the very different data sets used (Paα vs. Hα imaging, high vs. relatively low spatial resolution, circumnuclear vs. disk H II regions). This similarity may well indicate common physical processes underlying the massive SF in circumnuclear and disk areas in spiral galaxies.

The peak of the H II region LF, which corresponds to the lower luminosity end where the LF is complete, is relatively constant in these galaxies, and occurs at approximately $\log L(\mathrm{H}\alpha) = 37\,\mathrm{erg\,s^{-1}}$, a value similar to that found by Scoville et al. (2001) in M51. The one exception is IC 750, a galaxy which is not only interacting, but also by far the most distant of the galaxies discussed in this section. We find that the LFs of the circumnuclear H II regions extend to Hα luminosities of the order of $\log L(\mathrm{H}\alpha) = 38.3 - 38.8\,\mathrm{erg\,s^{-1}}$ in most cases, but the LFs cover luminosities of up to $\log L(\mathrm{H}\alpha) = 39.9\,\mathrm{erg\,s^{-1}}$ in those galaxies with enhanced SF (NGC 2903, NGC 6946 and IC 750). Ground-based LFs for disk H II regions usually extend out to $\log L(\mathrm{H}\alpha) \simeq 40\,\mathrm{erg\,s^{-1}}$ (e.g., KEH; Rozas et al. 1998a), although the high luminosity end depends upon the galaxy distance, as it is the case of our sample.

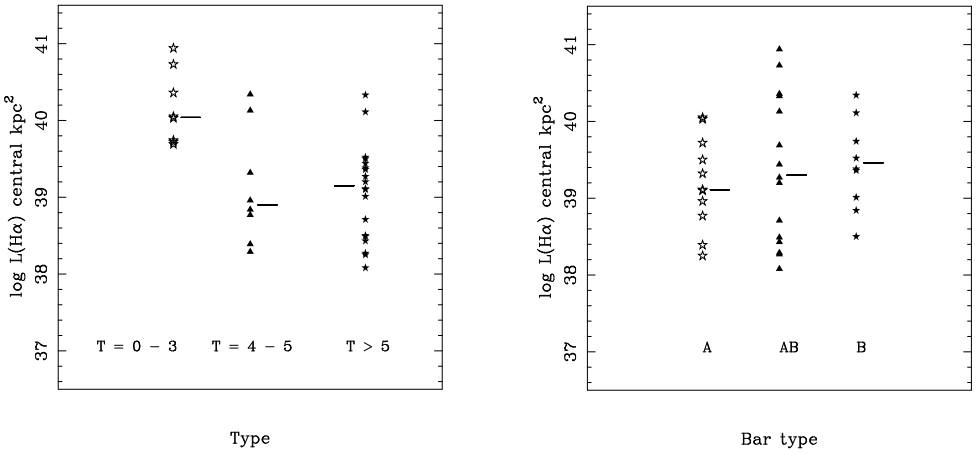

FIG. 4.— As Figure 2, but for the Hα luminosity in H II regions over the central kpc.

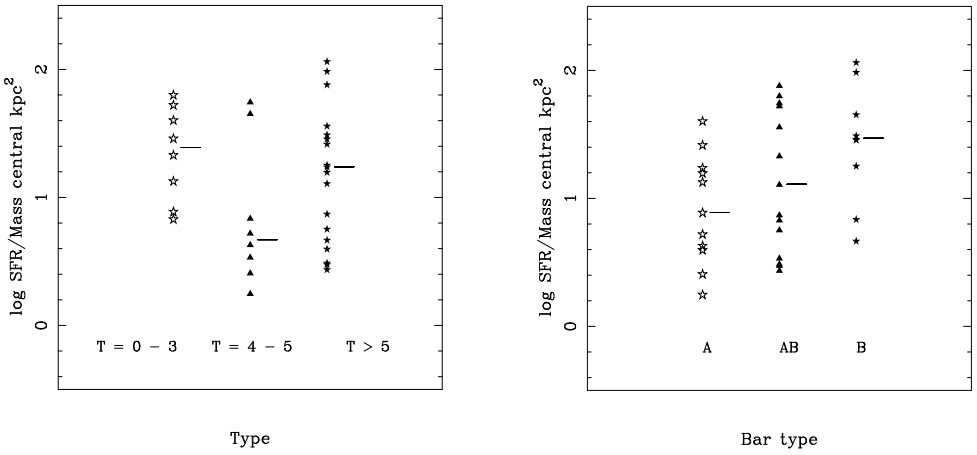

FIG. 5.— As Figure 2, but for the SFR per unit stellar mass over the central kpc.

TABLE 3
PARAMETERS OF THE FITTED H II REGION LF FOR SELECTED GALAXIES.

Galaxy	Type	α	$\log L(\mathrm{H}\alpha)$ range (erg s^{-1})
NGC 2903	SB(s)d	-1.65 ± 0.16	$37.5 - 39.5$
NGC 3077	I0pec	-1.70 ± 0.07	$36.7 - 38.3$
IC 750	Sab	-2.02 ± 0.07	$38.3 - 39.9$
NGC 3593	SA(s)0/a	-1.68 ± 0.16	$37.4 - 38.8$
NGC 4449	IBm	-1.85 ± 0.05	$36.7 - 38.5$
NGC 4826	(R)SA(rs)ab	-2.27 ± 0.16	$36.9 - 38.5$
NGC 5055	SA(rs)bc	-2.32 ± 0.18	$37.3 - 38.3$
NGC 6946	SAB(rs)cd	-1.83 ± 0.05	$36.9 - 39.5$

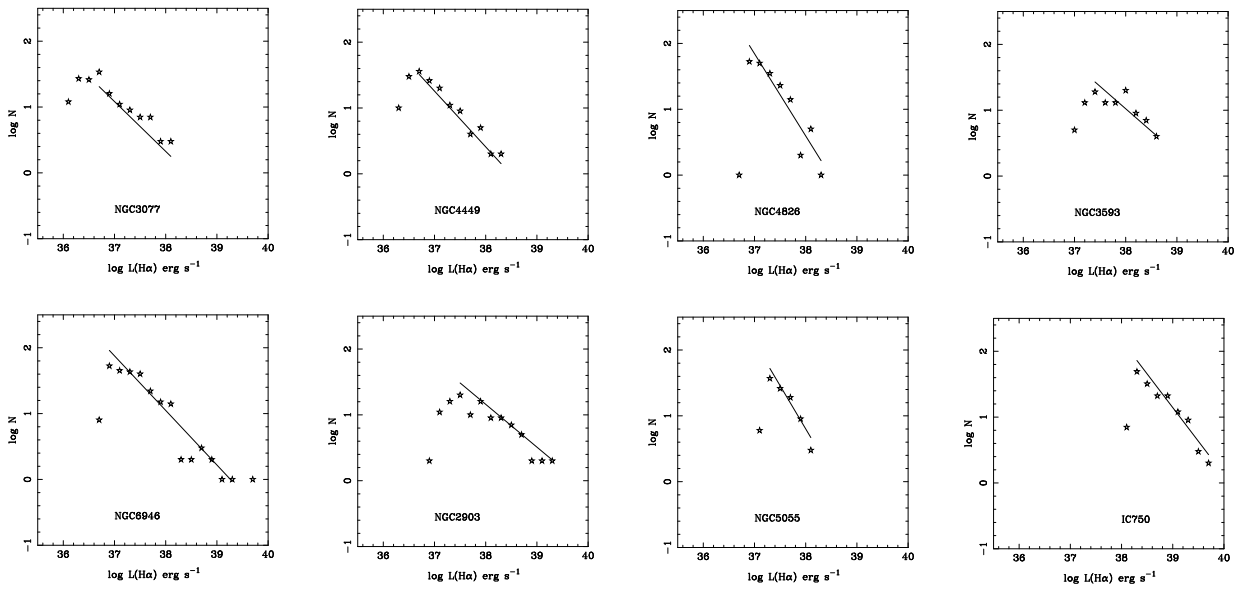

FIG. 6.— Luminosity Functions of galaxies with 100 or more H II regions, and power law fits.

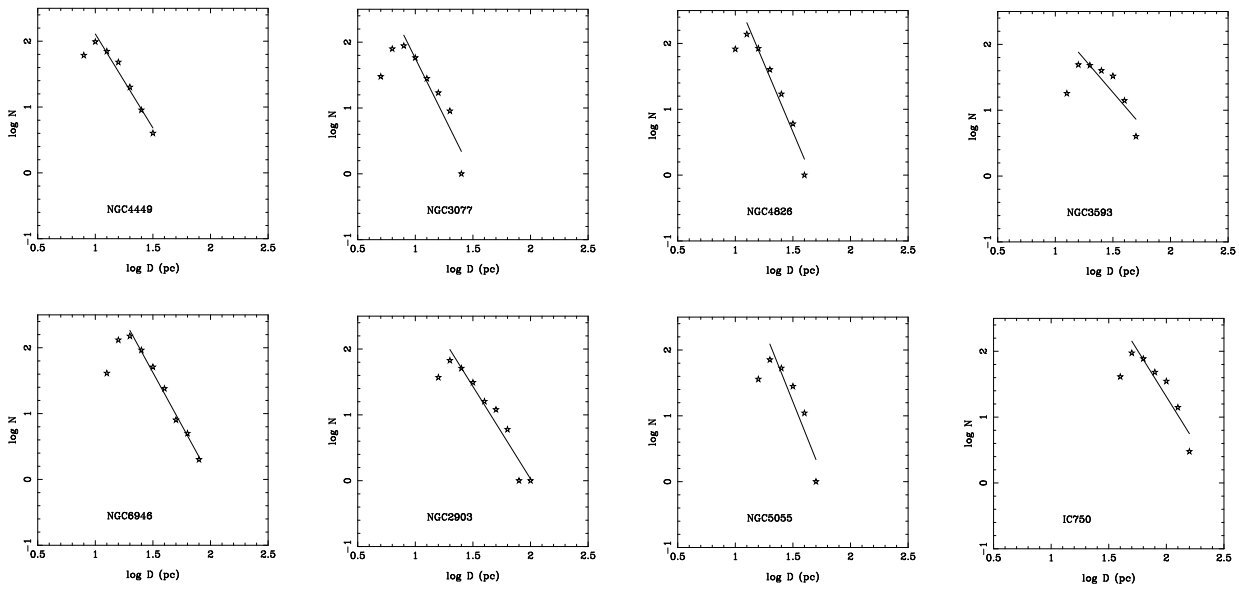

FIG. 7.— Differential diameter distributions of galaxies with 100 or more H II regions, and power law fits.

Although our numbers are small, we point out another effect, namely that the slopes of the circumnuclear H II region LFs tend to be shallower in later type galaxies, in good agreement with findings by KEH and Banfi et al. (1993) for disk H II regions. The only discrepant galaxy is NGC 3593. Oey & Clarke (1998) interpreted the steeper slopes in early type galaxies as due to a decrease in the upper limit to the number of stellar clusters. They based their argument on the claim by Caldwell et al. (1991) that Sa galaxies only show maximum Hα luminosities in the range $\log L(\mathrm{H}\alpha) = 38.0 - 38.5\,\mathrm{erg\ s^{-1}}$, and that they may thus only contain unsaturated clusters (clusters with poor stellar statistics). We have already shown above that that may not be the case for all early type galaxies. Other possibilities for the steeper LF slopes in early type galaxies would be a change in the slope of the stellar cluster distribution, or an aging effect.

In a series of studies of the properties of H II regions of grand design spiral galaxies, Beckman et al. (2000, and references therein) have pointed out the presence of a glitch in the LF at a luminosity of $\log L(\mathrm{H}\alpha) = 38.6 \pm 0.1\,\mathrm{erg\,s^{-1}}$, accompanied by a steepening of the slope of the LF for luminosities above this value. Beckman et al. interpreted this luminosity and other pieces of observational evidence to argue this luminosity marks the transition between ionization-bounded and density-bounded H II regions. This interpretation has, however, been disputed by Pleuss et al. (2000), who claim that the glitch in the LF, as well as some of the other observational hints, may be artifacts due to blending of H II regions as a direct result of the limited, ground-based, spatial resolution of the data used by Beckman et al. (2000). This is a debate that is outside the scope of this paper, but we do point out that there is no clear evidence for the presence of a glitch or change of slope near the luminosity reported by Beckman et al. (2000) from the circumnuclear H II region LFs in Figure 6. From our few LFs we do not find a change of slope at $\log L_(\mathrm{H}\alpha) = 38.6 \pm 0.1\,\mathrm{erg\,s^{-1}}$, presumable because with our *HST* imaging we resolve luminous H II regions into several less luminous ones. Scoville et al. (2001) report similar results from their *HST* study of H II regions in M51.

4.2. *Integral diameter distributions*

The integral diameter distribution of H II regions in galaxies is usually described as an exponential relation,

$$N(>D) = N_0 \mathrm{e}^{-D/D_0}, \qquad (2)$$

which thus relates the number N of H II regions with diameters larger than D to the diameter D, where D_0 is the characteristic size of the distribution (van den Bergh 1981; Hodge 1983; Rozas, Knapen & Beckman 1996b). However, as discussed by Kennicutt & Hodge (1986) for the case of ionization-bounded H II regions within a neutral medium of uniform density, one would expect the Strömgren radii to exhibit a power law distribution:

$$\mathrm{d}N(R) = B\,R^{2-3\alpha}\,\mathrm{d}R = C\,R^{\beta}\,\mathrm{d}R. \qquad (3)$$

Indeed, recently Pleuss et al. (2000), using high resolution (*HST*) data, have shown that the size distribution of H II regions in selected regions in M101 is better fitted with a power law than with an exponential relation. Moreover, these authors suggest that some of the previously fitted exponential forms to the integral diameter distributions might have been caused by spatial resolution effects.

Since the resolution of our data is comparable to that of Pleuss et al. (2000), we can address the question of whether the diameter distributions for those galaxies with 100 or more H II regions can be fitted with power laws. The distributions are presented in Figure 7, and the power law fits are given in Table 4. We confirm the result reported by Pleuss et al. (2000) that at high spatial resolutions the diameter distributions can be fitted as power laws, as expected for ionization-bounded H II regions. Also listed in Table 4 are the predicted values for the slope of the relation ($\beta_{\mathrm{pred}} = 2 - 3\,\alpha$, with the errors in β_{pred} computed as $\Delta\beta_{\mathrm{pred}} = 3\,\Delta\alpha$). From this table it can be seen that there is a relatively good agreement (to within the errors) between the fitted values of β and those predicted from the LF under the above assumption of a constant density. This good agreement is reflected in the well behaved luminosity-volume relations (not shown). We also performed exponential fits to the diameter distributions, and found that generally the power law and the exponential forms provided fits to diameters distributions of similar statistical significance. A caveat we must mention here, though, is the measurement of diameters for H II regions in the rather crowded circumnuclear areas under investigation in this paper is not straightforward.

5. CONCLUDING REMARKS

We have used *HST*/NICMOS Paα observations of a sample of nearby galaxies to analyze for the first time the properties of the circumnuclear H II regions at spatial resolutions ranging from 1 to 30 pc. Our sample was selected from the *HST*/NICMOS snapshot survey of nearby galaxies (in H and Paα) by Böker et al. (1999). It encompasses 52 galaxies with morphological types S0/a and later, and velocities $v \leq 1000\,\mathrm{km\,s^{-1}}$. The high spatial resolution of these observations overcomes some of the blending problems encountered by previous ground-based studies, and allows a detailed comparison of the properties of circumnuclear and disk H II regions. Kennicutt (1998a) provides an excellent review on the subject of the SF properties in galaxies, and the dependencies on different factors such as the Hubble morphological type, presence of bars, interactions, and gas content, for both disks and circumnuclear regions. However, most previous works on circumnuclear SF properties were based on integrated properties rather than on the study of the properties of the individual H II regions.

We briefly summarize our main results, classed in three categories, below.

5.1. *Relation to morphological type*

We find that the physical properties of individual circumnuclear H II regions, as represented by typical H II regions (median Hα luminosity and size) and by first ranked H II regions (the most luminous and the largest H II regions), are not strongly dependent on the morphological type of the host galaxy. Also, we find no relationship between the number of circumnuclear H II regions per unit area and the morphological type. The behavior of the physical properties of circumnuclear H II regions is in clear

TABLE 4
PARAMETERS OF THE FITTED SIZE DISTRIBUTIONS OF H II REGIONS IN SELECTED GALAXIES.

Galaxy	β	$\log D$ range (pc)	$\beta_{\rm pred}$
NGC 2903	-3.81 ± 0.24	$1.3 - 2.0$	-2.95 ± 0.18
NGC 3077	-4.53 ± 0.59	$0.9 - 1.4$	-3.10 ± 0.21
IC 750	-3.81 ± 0.48	$1.7 - 2.4$	-4.06 ± 0.21
NGC 3593	-3.04 ± 0.48	$1.2 - 1.7$	-3.04 ± 0.48
NGC 4449	-3.86 ± 0.21	$1.0 - 1.5$	-3.55 ± 0.12
NGC 4826	-5.15 ± 0.44	$1.1 - 1.6$	-4.75 ± 0.48
NGC 5055	-5.38 ± 0.87	$1.3 - 1.7$	-4.96 ± 0.54
NGC 6946	-4.11 ± 0.15	$1.3 - 1.9$	-3.49 ± 0.15

contrast with that of disk H II regions which tend to be larger, brighter and more numerous (per unit area) for late type spiral and irregular galaxies (Kennicutt 1988; KEH).

Whereas the morphological type does not seem to be one of the dominant factors in determining the physical properties of the individual circumnuclear H II regions, it does influence the global circumnuclear SF properties. The Hα luminosities over the central kpc (only based upon emission from H II regions) are significantly enhanced in early-type (S0/a–Sb) galaxies when compared with late-type galaxies. This confirms the findings of Böker et al. (1999) for the average central surface Paα brightnesses (H II region and diffuse emission) over the field of view of the images, and other studies based upon optical spectroscopy (e.g., Ho et al. 1997a,b and references therein). When the SFR per unit stellar mass are compared with the morphological type, the trend disappears because it is offset by a trend in the opposite direction, where earlier type galaxies tend to have more massive bulges than later type galaxies.

5.2. *Relation to bars*

A relation between the presence of a bar and the properties of the circumnuclear SF is expected since bars are predicted to provide an efficient mechanism to transport gaseous material from the disks of galaxies into the central regions, and as a consequence bars may trigger the SF in the circumnuclear regions of galaxies. Indeed, barred galaxies have enhanced Hα luminosities (mostly occurring in early type galaxies) and SFR per unit stellar mass (or integrated pseudo equivalent width of Paα) over the central 1 kpc area when compared to unbarred galaxies. Whereas the number of H II regions per area or per unit stellar mass are not enhanced in barred with respect to non-barred galaxies, the first-ranked H II regions (both in terms of diameter and luminosity) are on average more luminous and larger in barred than in unbarred galaxies. This in conjuction with results from many other works provide further evidence that bars are efficient in triggering the SF in the central regions of galaxies, although, as pointed out among others by Ho et al. (1997b), the presence of a bar is neither a necessary nor a sufficient condition for SF to occur.

5.3. *LFs and diameter distributions*

We have analyzed the LFs and integral diameter distributions of the eight galaxies in our sample with one hundred or more circumnuclear H II regions. The LFs of the circumnuclear H II regions extend to Hα luminosities of $\log L({\rm H}\alpha) = 38.3 - 38.8\,{\rm erg\,s^{-1}}$, whereas in galaxies with enhanced SF the LFs reach $\log L({\rm H}\alpha) = 39.7\,{\rm erg\,s^{-1}}$. We fitted power law slopes of the circumnuclear H II region LFs, of between $\alpha = -2.3$ and $\alpha = -1.7$, values which are exactly within the range of slopes reported for spiral disks from ground-based observations (e.g., KEH). This suggests that the physical processes determining the massive SF in disks and circumnuclear regions must be common. Although we can only fit slopes to the H II region LFs for a very limited number of galaxies, we do confirm the relation between LF slope and galaxy type, with late type galaxies showing shallower LFs.

The integral diameter distributions for these eight galaxies are fitted with power laws whose indices are in a relatively good agreement with those predicted from the LF, assuming that the H II regions are ionization-bounded within a medium of uniform density. We find, however, that the more commonly used exponential form provides fits of similar statistical significance.

5.4. *Final comments*

With the detailed analysis of narrow band Hα and Paα images of spiral galaxies obtained with the *HST*, we have recently entered a new era in research on extragalactic H II regions (Pleuss et al. 2000; Scoville et al. 2001; this paper). One of the main conclusions from all these works is that although blending may affect results based on ground-based narrow-band imaging, one of the main parameters describing statistical ensembles of H II regions from *HST* data, namely the slope of the LF, is still within the previously observed values. The recent conclusions emerging from studies using *HST* imaging, which are based either on partial imaging of the disk of one individual galaxy, or, as in our case, on imaging of the circumnuclear parts only of a sample of spiral galaxies, will need to be confirmed by more extensive studies using high-resolution narrow-band imaging, but contain important clues to the underlying

physical processes of massive SF in galaxies.

ACKNOWLEDGMENTS

We are grateful to an anonymous referee for useful comments that helped improve the paper. It is a pleasure to thank Dr. C. H. Heller for providing us with the REGION software, used to analyze the properties of the H II regions, and Drs. J.E. Beckman and A. Zurita for comments on an earlier version of the manuscript.

This research has made use of the NASA/IPAC Extragalactic Database (NED) which is operated by the Jet Propulsion Laboratory, California Institute of Technology, under contract with the National Aeronautics and Space Administration.

REFERENCES

Alonso-Herrero, A., Rieke, G. H., Rieke, M. J., & Scoville N. Z. 2000, ApJ, 532, 845
Balzano, V.A., 1983, ApJ, 268, 602
Banfi, M., Rampazzo, R., Chincarini, G., & Henry, R. B. C. 1993, A&A, 280, 373
Beckman, J. E., Rozas, M., Zurita, A., Watson, R. A. & Knapen, J. H. 2000, AJ, 119, 2728
Böker, T. et al., 1999, ApJS, 124, 95
Caldwell, N., Kennicutt, R. C. Jr., Phillips, A. C., & Schommer, R. A. 1991, ApJ, 370, 526
Cepa, J., & Beckman,,J. E. 1989, A&AS, 79, 41
Cepa, J., & Beckman, J. E. 1990, A&AS, 83, 211
Devereux, N. 1987, ApJ, 323, 91
Devereux, N. A., & Hameed, S. 1997, AJ, 113, 599
Eisenhauer, F. 2001, in Tacconi, L.J., Lutz, D., eds, Starbursts: Near and Far, Springer, in press
Elmegreen, B.G. 1999, in Beckman J. E., Mahoney T. J., eds, The Evolution of Galaxies on Cosmological Timescales. Astron. Soc. Pac., San Francisco, Vol. 187, 145
Feinstein C., 1997, ApJS, 112, 29
Gilmore, G. 2001, in Tacconi, L.J., Lutz, D., eds, Starbursts: Near and Far, Springer, in press
Hameed, S., & Devereux, N. 1999, AJ, 118, 730
Heckman, T.M. 1980, A&A, 88, 365
Ho, L. C., Filippenko, A. V., & Sargent, W. L. W. 1997a, ApJ, 487, 579
Ho, L. C., Filippenko, A. V., & Sargent, W. L. W. 1997b, ApJ, 487, 591
Hodge, P. 1969, ApJS, 18, 73
Hodge, P. 1974, PASP, 86, 845
Hodge, P. 1983, AJ, 88, 1323
Hodge, P. 1986, PASP, 98, 1095
Kennicutt, R. C. Jr. 1986, ApJ, 306, 130
Kennicutt, R. C. Jr. 1988, ApJ, 334, 144
Kennicutt, R. C. Jr. 1998a, ARA&A, 36, 189
Kennicutt, R. C. Jr. 1998b, ApJ, 498, 541
Kennicutt, R. C. Jr., & Kent, S. M. 1983, AJ, 88, 1094
Kennicutt, R. C. Jr., Edgar, B. K., & Hodge, P. W. 1989, ApJ, 337, 761 (KEH)
Kingsburgh, R. L., & McCall, M. L. 1998, AJ, 116, 2246
Knapen, J. H. 1998, MNRAS, 297, 255
Knapen, J. H., Arnth-Jensen, N., Cepa, J., & Beckman, J. E. 1993, AJ, 106, 56
Knapen, J. H. 1999, in Beckman J. E., Mahoney T. J., eds, The Evolution of Galaxies on Cosmological Timescales. Astron. Soc. Pac., San Francisco, Vol. 187, 72
Maiolino, R., Alonso-Herrero, A., Anders, S., Quillen, A., Rieke, M. J., Rieke, G. H., & Tacconi-Garman, L. E. 2000, ApJ, 531, 219
McKee, C. F., & Williams, J. P. 1997, ApJ, 476, 144
Oey, M. S., & Clarke, C. J. 1997, MNRAS, 289, 570
Oey, M. S., & Clarke, C. J. 1998, AJ, 115, 1543
Osterbrock, D. E. 1989, in Astrophysics of Gaseous Nebulae and Active Galactic Nuclei, University Science Books, Mill Valley, California
Pleuss, P. O., Heller, C. H., & Fricke, K. J. 2000, A&A, 361, 913
Rand, R. J. 1992, AJ, 103, 815
Rieke, G. H., & Lebofsky, M. J. 1985, ApJ, 288, 618
Rozas, M., Beckman, J. E., & Knapen, J. H. 1996a, A&A, 307, 735
Rozas, M., Beckman, J. E., & Knapen, J. H. 1996b, A&A, 312, 275
Rozas, M., Zurita, A., Heller, C. H., & Beckman, J. E. 1999, A&AS, 135, 145
Scoville, N. Z., Polletta, M., Ewald, S., Stolovy, S. P., Thompson, R., & Rieke, M. 2001, submitted to AJ
Shlosman, I., Begelman, M. C., & Frank, J. 1990, Nature, 345, 679
Strömgren, B. 1939, ApJ, 89, 526
Thilker, D. A., Braun, R., & Walterbos, R. A. M. 2000, AJ, 120, 3070
Thronson, H. A., & Greenhouse, M. A. 1988, ApJ, 327, 671
Tully, R. B. 1988, Nearby Galaxies Catalogue (NBG), Cambridge University Press
van den Bergh, S. 1981, AJ, 86, 1464
von Hippel, T., & Bothun, G. 1990, AJ, 100, 403
Walterbos, R. A. M., & Braun, R. 1992, A&AS, 92, 625
Wyder, T. K., Hodge, P. W., & Skelton, B. P. 1997, PASP, 109, 927